Accepted Manuscript

Multi-Walled Carbon Nanotube-Coated Spiral Coils for Loss Reduction in Wireless Power Transfer Systems

Kamran Keramatnejad, Dawei Li, Hossein Rabiee Golgir, Loic Constantin, Xi Huang, Qiming Zou, Jean-Francois Silvain, Stephen Ducharme, Yongfeng Lu

PII: S0008-6223(18)30669-9

DOI: 10.1016/j.carbon.2018.07.027

Reference: CARBON 13308

To appear in: *Carbon*

Received Date: 11 February 2018

Accepted Date: 10 July 2018

Please cite this article as: Kamran Keramatnejad, Dawei Li, Hossein Rabiee Golgir, Loic Constantin, Xi Huang, Qiming Zou, Jean-Francois Silvain, Stephen Ducharme, Yongfeng Lu, Multi-Walled Carbon Nanotube-Coated Spiral Coils for Loss Reduction in Wireless Power Transfer Systems, *Carbon* (2018), doi: 10.1016/j.carbon.2018.07.027

Multi-Walled Carbon Nanotube-Coated Spiral Coils for Loss Reduction in Wireless Power Transfer Systems

Kamran Keramatnejad [a], Dawei Li [a], Hossein Rabiee Golgir [a], Loic Constantin [a], Xi Huang [a], Qiming Zou [a], Jean-Francois Silvain [b], Stephen Ducharme [c], and Yongfeng Lu [a,1*]

[a]Department of Electrical and Computer Engineering, University of Nebraska-Lincoln, Lincoln, NE 68588-0511, United States

[b]Institut de Chimie de la Matière Condensée de Bordeaux, Avenue du Docteur Albert Schweitzer F-33608 Pessac Cedex, France

[c]Department of Physics and Astronomy, Nebraska Center for Materials and Nanoscience, University of Nebraska-Lincoln, Lincoln, NE 68588-0299, United States

*Corresponding author.
E-mail address: ylu2@unl.edu, phone number: +01-402-4728323 (Y.F. Lu)

Abstract

Realization of high efficiency and long transmission range in high-frequency wireless power transfer (WPT) systems has always been hindered by the increased resistance due to the eddy current loss occurring in the inductive coils. In this study, multi-walled carbon nanotube-coated copper (MWCNT-Cu) coils are successfully introduced to address this limitation by implementing the frequency-inert MWCNT channels along with using their high-surface areas to realize the electromagnetic shielding of the Cu substrate through multiple reflection mechanisms. At a frequency of 15 MHz, the resistance of the individual MWCNT-Cu coil was reduced to less than 40% of its original value for primitive Cu, leading to more than a four-fold increase in their quality factor. When MWCNT-Cu coils were used as the transmitting component, the transmission efficiency of the WPT system increased from 10.57% to 95.81% at a transmission distance of 4 cm and a frequency of 3.45 MHz. Finally, it was demonstrated that the loss reduction improved as the eddy current loss became more severe in coils with higher inductance values, which makes this approach promising for significantly improving the performance of inductive components in WPT applications.

1. Introduction

The development of wireless power transfer (WPT) systems based on magnetic resonance coupling has received increasing attention in recent years due to their promising potential applications such as wireless charging,[1-3] radio-frequency identification (RFID),[4] and biomedical microelectronics.[5-7] According to C95.1-2005-IEEE Standard, the MHz range frequency is required to be incorporated in the design process of the WPT system, in order to reduce risks deriving from human/animal exposure.[8] This, however, leads to increased AC resistance in conventional copper (Cu) coils due to skin- and proximity-effect losses, thereby limiting the power transmission efficiency and effective range of WPT systems.[9-13] To address this limitation, several approaches have been proposed for the fabrication of inductive coils, such as using Litz-wires,[14-16] magnetoplated wire,[17] and planar spiral winding (PSW). However, the impact of these approaches is limited to KHz frequencies.[12, 18] In addition, they add a considerable amount of complexity to the fabrication process and are not scalable.

Multi-walled carbon nanotubes (MWCNTs) have attracted a great deal of attention due to their outstanding properties, specifically in high-frequency (HF) applications.[19-24] In particular, the high conductivity and permeability of MWCNTs, along with their high aspect ratio and exceptional mechanical strength, compared to their carbon-based counterparts such as graphene nanoplatelets, make them promising candidates for electromagnetic shielding through intensification of the multiple internal reflection mechanism.[25-29] In addition, as highlighted in previous reports, the AC conductivity of MWCNTs remains relatively unchanged with respect to the varying magnetic field due to their large momentum relaxation time,[21, 22, 30-32] thereby making their electrical performance almost independent of the frequency.

In this work, we propose the fabrication of MWCNT coatings on the surface of Cu coils *via* the electrophoretic deposition (EPD) method, in order to prevent the deflection of current density in Cu by forming a highly conductive, frequency-independent electrical channel. At the same time, MWCNT coatings can attenuate the external electromagnetic field in the vicinity of the adjacent turns in the Cu coils, preventing the deflection of current density in Cu and thereby suppressing loss due to the proximity effect. The impedance characteristics of individual MWCNT-coated Cu (MWCNT-Cu) coils were studied and compared to those characteristics prior to the deposition of MWCNTs. In addition, the impact of MWCNT coating on the transmission efficiency parameters of the WPT system was investigated by using the MWCNT-Cu coils as transmitters.

2 Experimental section

2.1 Sample preparation

Fig.1a shows the schematic diagram of the EPD system used for the formation of the MWCNT coatings on the surface of the Cu coils. The coils were fabricated by bending a Cu piping with a 6-mm outer diameter and a 1-mm wall thickness. According to previous theoretical and experimental studies, the internal reflection of the electromagnetic field and the AC conductivity of the MWCNT coatings is in direct relation with their aspect ratio.[25, 30, 33, 34] In addition, their surface area, which is crucial in electromagnetic shielding, is inversely proportional to their diameter. Therefore, we aimed to use MWCNTs with the highest aspect ratio of equal to 8000 (smallest diameter ~ 5nm, highest length ~ 40 μm) which were commercially available in order to realize the best electrical performance and the highest electromagnetic shielding in MWCNT-Cu coils. Moreover, the EPD parameters were chosen in a way to minimize the porosity and accordingly to avoid inter-tube resistance in the fabricated MWCNT coating. A 1g/L MWCNT solution was prepared by dispersing MWCNT powder (Cheap Tubes, Inc) uniformly into 1, 2-Dicholoroethane (DCE) (Sigma-Aldrich, Inc) followed by sonication for 2 hours. The Cu coils were then submerged in the MWCNT-DCE solution acting as the cathode, while a cylindrical thin copper foil was used as the anode. The deposition of MWCNTs was then carried out under a DC applied voltage of 25 V for 10 min. Next, the MWCNT-Cu coils were dried out at 250°C under vacuum conditions for 2 hours.

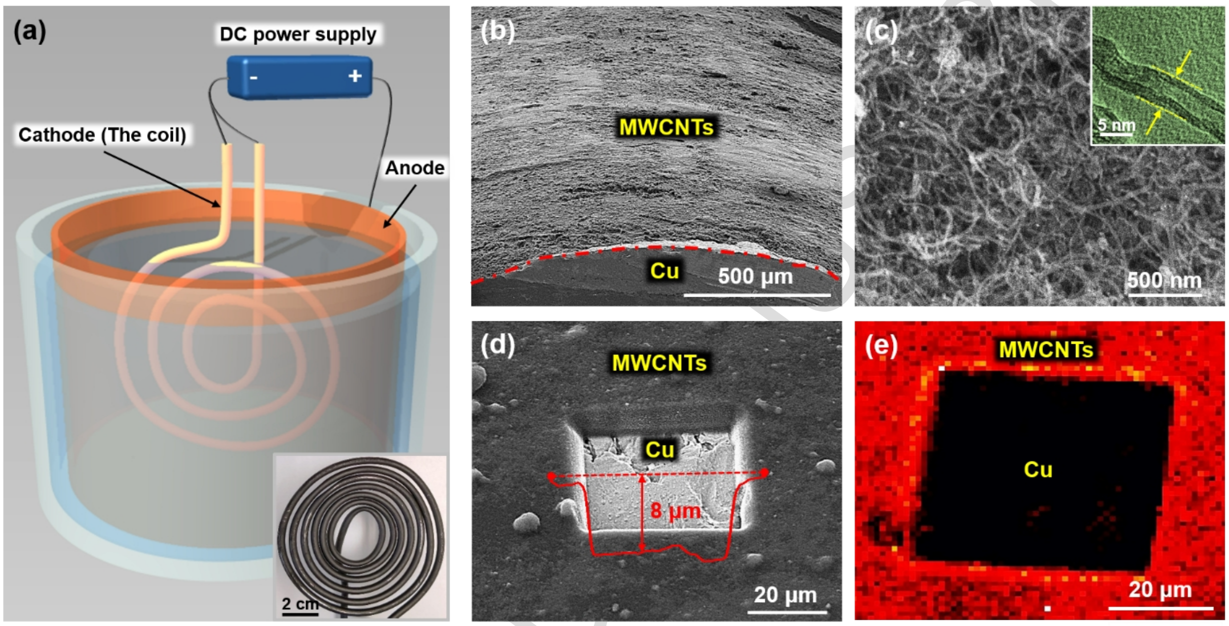

Fig. 1. Fabrication and characterization of MWCNT-Cu spiral coils. (a) Schematics of the EPD setup. Inset shows the top-view photograph of the MWCNT-Cu coil used as the transmitter coil. (b) Cross-sectional SEM image of the MWCNT-Cu spiral coil sample. (c) Top view SEM image of the deposited MWCNTs. The inset shows a typical TEM image of a single MWCNT with inner and outer diameters of ~ 2 nm and ~ 5 nm, respectively. (d) Angled view SEM image taken from the surface of the MWCNTs partially etched away *via* fs laser etching. The red solid line shows the thickness profile along the width of the etch area (red dashed line). (e) Raman mapping of G-band peak intensity obtained at the area shown in (d).

2.2 Characterization

Structural properties of the MWCNTs were investigated using Field emission scanning electronic microscope (FESEM, Hitachi S4700), transmission electron microscope (JEM 2010, JEOL, Japan), and optical surface profiling system (Zygo NewView 8300). Room-temperature Raman spectral analysis was performed using a micro-Raman spectrometer (Renishaw inVia™ Plus, Renishaw). An argon ion laser (λ = 514 nm) with an output power of 3.0 mW was used as the excitation source, and the spectra was collected using a ×50 objective lens with an accumulation of 1.0 s per position. Four-point probe measurements were, indeed, carried out for all of the fabricated MWCNT coatings in order to compare their DC conductivity with previously reported results, monitor their quality, and check the repeatability and reproducibility of the EPD step. These measurements were carried out using an Agilent 4155C semiconductor parameter analyzer connected to a probe station (Cascade Microtech, MPS150) equipped with HVP probes. The AC performance of the MWCNT-Cu coils was studied using an impedance Analyzer (HP, 4192A). All the samples were characterized at 0 < f < 15 MHz frequency range which covers all the values applied to the design of the recent large-scale and sub-meter gap WPT systems.[17, 35-37] In addition, a wide-bandwidth (500 MHz) digital storage oscilloscope (TDS3052B Tektronix, Inc) was used to analyze the steady-state power transmission efficiency characteristics of the MWCNT-Cu-coil-based WPT systems. The parasitic contact resistance between the coils and the power probes was measured and de-embedded from the collected data in all of the measurements.

3 Results and discussion

3.1 Structural analysis

Fig. 1b depicts the field emission scanning electron microscopy (FESEM) image taken at the cross-section of the MWCNT-Cu spiral coil, where MWCNT coatings were uniformly formed on the surface of the Cu coils *via* the EPD method. A closer view of the MWCNTs in Fig. 1c reveals that the coating appears to have an intertwined structure. The void fraction ($\phi = \frac{V_{Void}}{V_{Total}} \times 100$) [38] calculated from void volumes V_{Void} and the total MWCNT volume V_{Total} of the composite for all of the samples was ~ 26 %. This is of considerable importance because the high conductivity of the MWCNT coating is essential, as it both provides a low-resistance channel on the surface of the coil and shields it from magnetic interference from the adjacent turns.[39, 40] The measured DC conductivity of the samples studied range between 244000 and 333000 S/cm which is close to previously reported values obtained from numerical simulations.[30] On the basis of the TEM observation (inset in Fig. 1c), the inner and outer diameters of MWCNTs can be estimated to be ~

2 nm and ~ 5 nm, respectively. The thickness of the MWCNT coatings was studied through femtosecond (fs) laser ablation of MWCNTs at a given area (see the Experimental section), as depicted in Fig. 1d. The thickness of the MWCNT coating was observed to be around 8 μm at which the most uniform coating was obtained. Fig. 1e shows the Raman intensity mapping of the G-band obtained at the vicinity of the laser-ablated area in Fig. 1d, further confirming the uniformity of the MWCNT coating.

3.2 Characteristics of individual MWCNT-Cu coils

Fig. 2a shows the eddy current-induced AC resistance (R_{AC}) of a coil before and after the formation of the MWCNT coating on Cu foils. As expected of Cu conductors, the magnitude of R_{AC} monotonically increased as a function of the frequency (f) due to the copper losses. However, the R_{AC} value was reduced for the MWCNT-Cu coil and became less dependent on the frequency, indicating the mitigation of the proximity effect. Specifically, the R_{AC} value of the MWCNT-Cu coil was reduced to 60% of its original value at a frequency of 15 MHz. As shown in Fig. 2b, the inductance value (L) of the MWCNT-Cu coils increased by more than 50% of its original value at f = 15 MHz, thereby increasing its quality factor by four fold. In fact, these improvements were in direct relation with f (Fig. 2c). The percentage reduction of the R_{AC} of the MWCNT-Cu coils compared to ordinary ones (calculated at f = 15 MHz) can be calculated by:

$$\Delta = \frac{R_{AC,Cu} - R_{AC,MWCNT-Cu}}{R_{AC,Cu}} \times 100. \qquad (1)$$

where $R_{AC,Cu}$ and $R_{AC,MWCNT\text{-}Cu}$ are the AC resistance of the coils before and after the formation of the MWCNT coating, respectively. The Δ value for a number of coils studied in this work is illustrated in Fig. 2d with results indicating a positive value. In addition, it was noticed that Δ value tended to increase as the number of turns (N) and, accordingly, the L value increased. It is known that the proximity effect becomes more significant and leads to a considerable increase in the R_{AC} value as the L value increases.[41] Therefore, the direct relation between the Δ value and the L value in Fig. 2d demonstrates the effectiveness of the proposed approach in reduction of the eddy current-induced power loss as it becomes more severe in coils with higher inductance values.

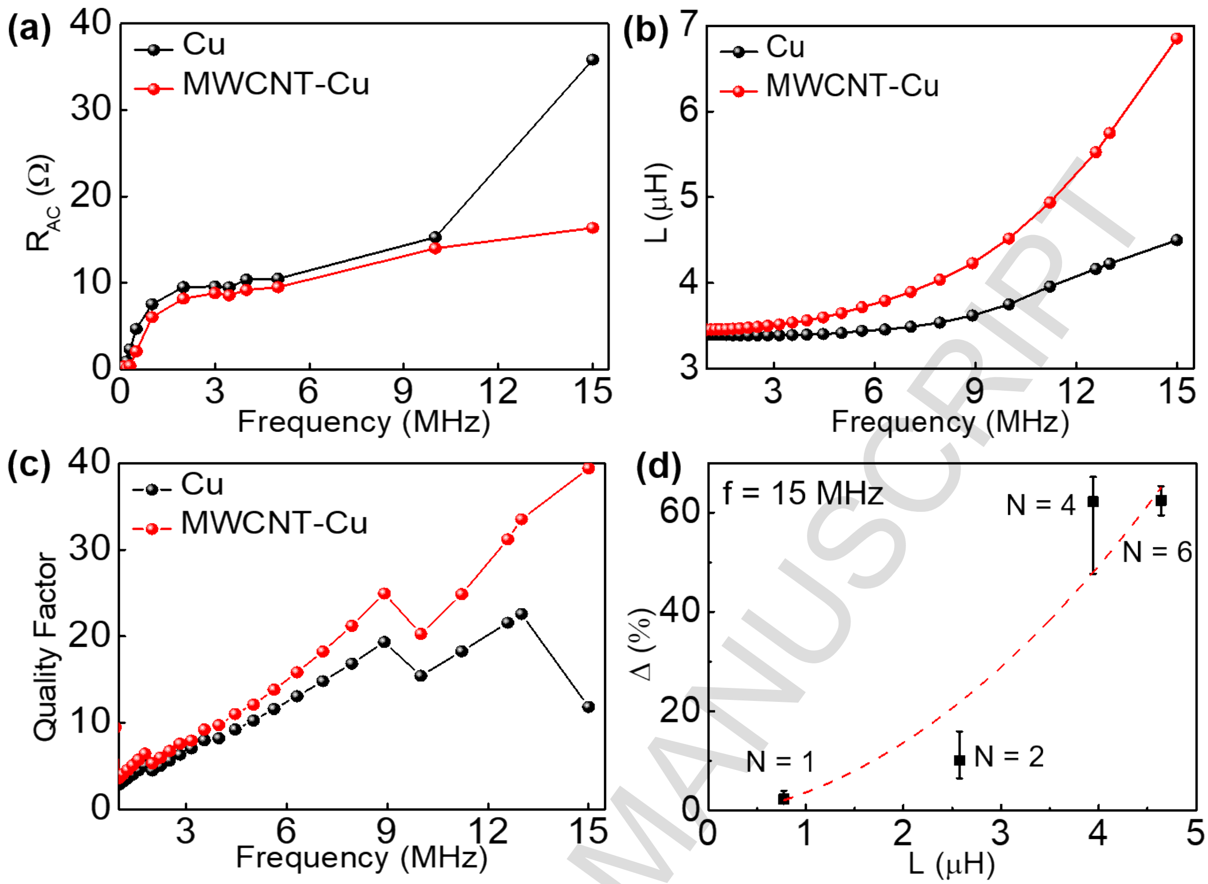

Fig. 2. (a) R_{AC}, (b) L, and (c) the quality factor as functions of frequency for the Cu spiral coil before (black line) and after (red line) the formation of MWCNT coatings. (d) The calculated percentage Reduction (Δ) of the R_{AC} vs L along with its experimental uncertainties. Note that f = 15 MHz was chosen since the proximity effect was significant and measurable for all of the samples at this frequency.

Based on the results obtained from the electrical measurements, it was evident that the R_{AC} of the MWCNT-Cu coils was significantly reduced due to the suppression of the copper loss, by forming a low-resistance, frequency-independent MWCNT layer on Cu surface, where the MWCNTs provided an auxiliary conduction channel with a frequency-independent conductivity, as qualitatively illustrated in Fig. 3a. Both theoretical and experimental studies have proven that high aspect ratio in MWCNTs leads to large electrical conductivity.[25, 33] The one-dimensional structure of the MWCNTs increases the probability to reduce the inter-tube gaps and accordingly contribute to a highly conductive network of MWCNTs. In addition, the aspect ratio is in direct relation with the surface area of the MWCNT coating, which is essential for the attenuation of the external magnetic field and suppressing the proximity effect. Therefore, the large surface area of the MWCNTs helps intensify the internal reflection of the electromagnetic field induced by the varying current in neighboring turns, preventing the redistribution of the internal current and, thereby, suppressing the proximity effect (Fig. 3b).

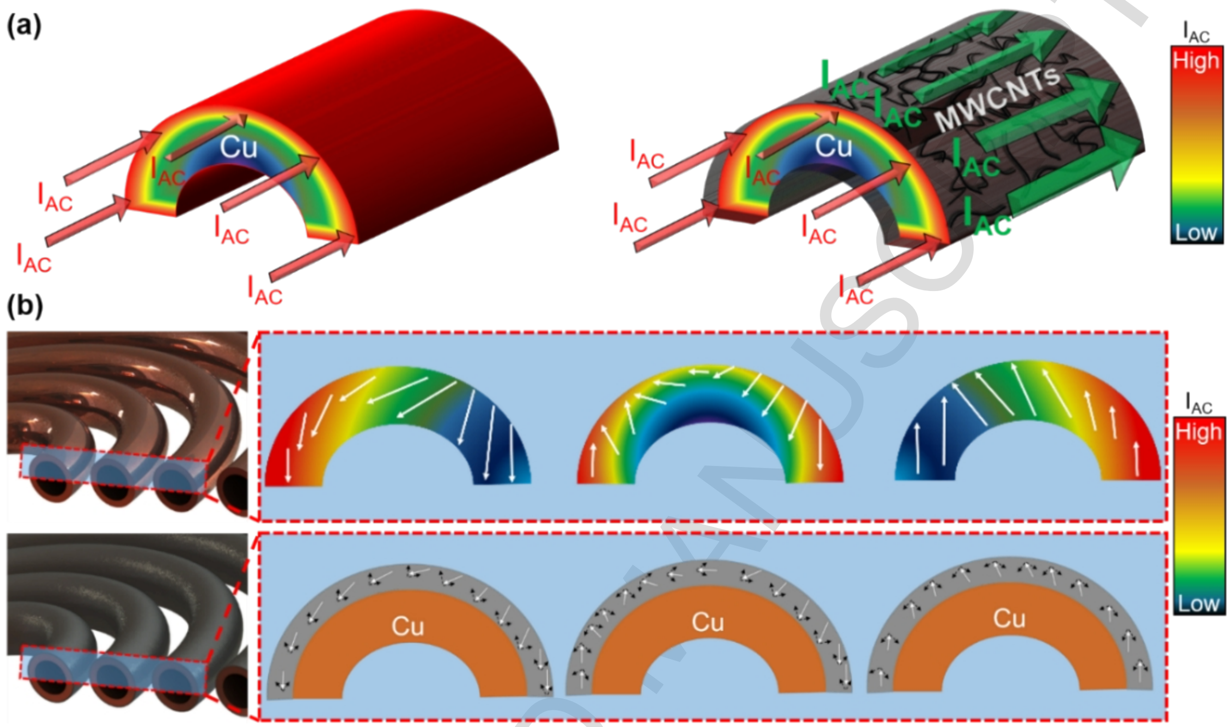

Fig. 3. (a) A qualitative comparison of the skin-effect-induced current distribution between the Cu (left) and MWCNT-Cu (right) coils in a single turn, where the red arrows represent the deflected current density in the metal substrate and the green arrows represent the added current density in the MWCNT channel. (b) Cross-sectional schematic diagram and the corresponding proximity effect-induced field redistribution in the Cu coil (top) and MWCNT-Cu coil (bottom). Note that the white arrows represent the external electromagnetic field incident upon each conductor.

3.3 Characteristics of WPT system including MWCNT-Cu coils as transmitters

Fig. 4a and b show the photograph and equivalent circuit of the WPT system used in this study, respectively. The coils were installed on an adjustable test bed in order to change the air gap distance (X) between the transmitting and receiving coils (Fig. 4a). As shown in Fig. 4b, the coils were modeled as lumped inductors in series with a resistance representing the overall parasitic losses caused by skin- and proximity-effects. C_t and C_r represent the primary and secondary series resonance capacitors, respectively, which are used to maximize the efficiency of the WPT system. The value of these capacitors can be calculated by:

$$C = \frac{(2\pi f_{Resonance})^2}{L}. \quad (2)$$

where f = 3.45 MHz is the resonance frequency and L is the inductance value of each coil. To investigate the impact of the MWCNT-Cu coils as transmitter components on the performance of a WPT system, we measured and compared the power transmission efficiency of WPT systems based on MWCNT-Cu coil and bare Cu coil under various conditions (Fig. 4c-f). It should also be pointed out that the input power was kept constant (~ 0.5 W), and a similar receiver coil was used for all of the experiments.

Fig. 4c compares the measured η value of the WPT system (at X = 4 cm) as a function of the load resistance (R_L) for a given coil (L_{t1} = 4.640 μH) before and after the formation of MWCNT coating on Cu coils. We found that efficiency degrades with the increase in R_L, which is expected for all classes of WPT systems.[42-44] Compared to bare Cu coil, an overall increase in the η value was observed when the MWCNT-Cu coil was used as the transmitter coil. In particular, the efficiency of the WPT system based on MWCNT-Cu coil at R_L = 3 Ω was calculated to be ~ 95.81 %, which is much higher than the one based on bare Cu foil (~ 10.57 %). The efficiency improvement was also observed in similar experiments conducted for a variety of coils. We then calculated the ratio of the transmission efficiency for the case where MWCNT-Cu coils were used to its pristine value ($\frac{\eta_{MWCNT-Cu}}{\eta_{Cu}}$) at R_L = 10 Ω (Fig. 4d). The direct relation between the $\frac{\eta_{MWCNT-Cu}}{\eta_{Cu}}$ ratio and the L value further suggests the successful suppression of the copper losses in MWCNT-Cu coils, which reportedly tend to become more severe in higher inductances due to the intensification of the electromagnetic field around the coils.

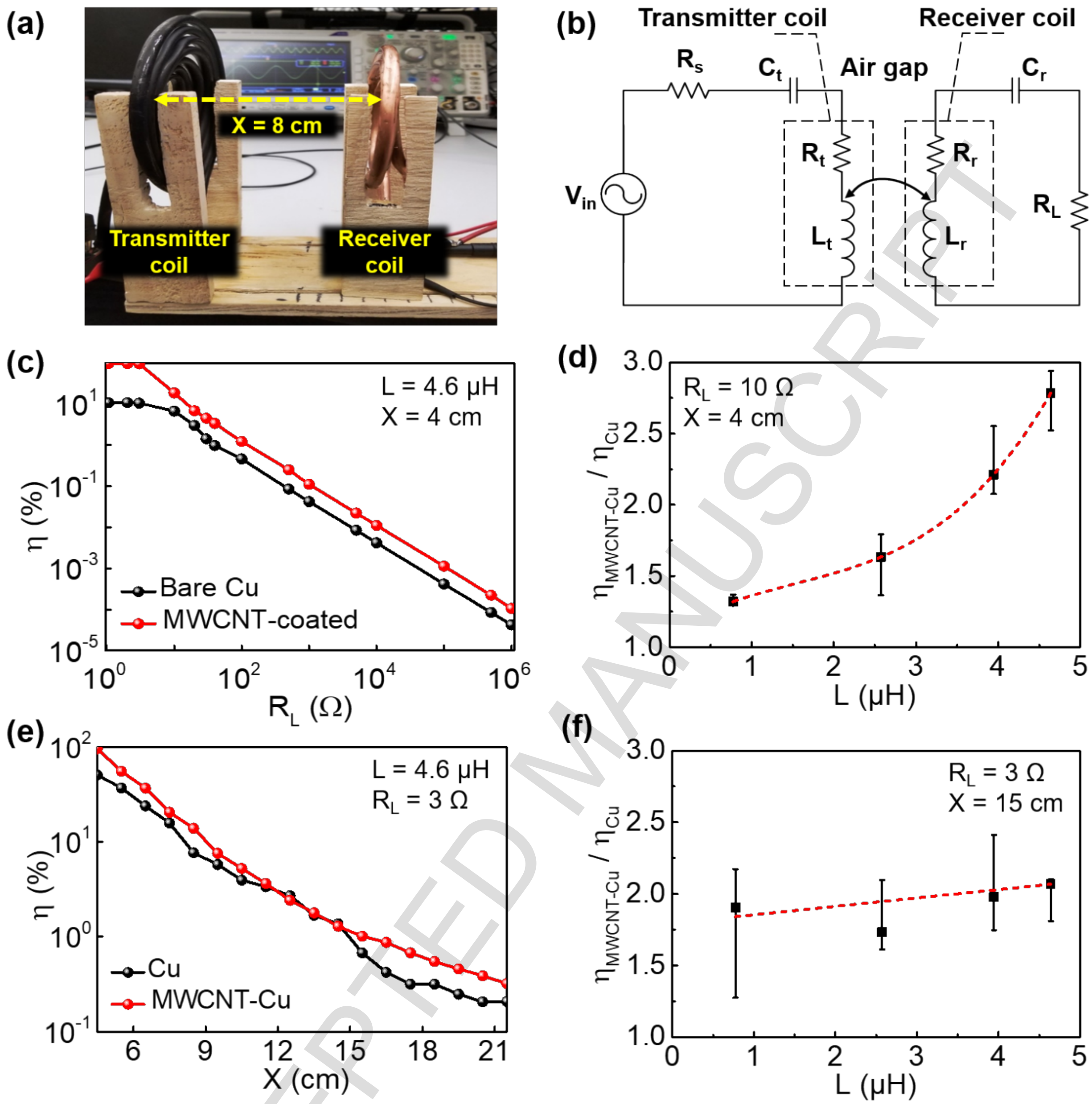

Fig. 4. (a) Photograph of the aligned WPT system using MWCNT-Cu spiral coil as the transmitter coil. (b) Equivalent circuit of the WPT system. (c) Transmission efficiency vs. R_L. (d) The calculated $\frac{\eta_{MWCNT-Cu}}{\eta_{Cu}}$ as a function of L at X = 4 cm. (e) Transmission efficiency vs. distance (X). (f) $\frac{\eta_{MWCNT-Cu}}{\eta_{Cu}}$ as a function of L at X = 15 cm. All of the experiments were carried out at f = 3.45 MHz.

Fig. 4e shows the efficiency of the aforementioned transmitter coil (L_{t1} = 4.640 μH) as a function of the air gap distance (X) before and after the formation of the MWCNT coating. It was observed that the efficiency was in reverse relation with X, which can be attributed to the degradation of the magnetic coupling between the transmitter and receiver coils. However, the η value of the WPT system based on MWCNT-Cu coil was slightly increased, particularly for X > 14 cm. At the distance (X) of 17 cm, a two-fold increase in the efficiency was observed due to the presence of the highly conductive MWCNTs, leading to the reduction in AC resistance. In addition, a direct relationship between the calculated $\frac{\eta_{MWCNT-Cu}}{\eta_{Cu}}$ ratio and the L value was observed (Fig. 4f), where the larger the L value, the higher the improvement in the transmission efficiency. This indicates that the proposed method is effective in increasing the available transmission range through suppression of the proximity effect, which is reportedly significant in WPT systems, including coils with large L values.[45-47]

4 Conclusions

In conclusion, we have successfully fabricated uniform, dense, and highly conductive MWCNT layers on the surface of Cu coils in order to suppress the copper loss in MHz WPT systems, where MWCNTs performed as an alternative frequency-independent electrical channel, leading to the suppression of the skin effect in Cu coils. A four-fold increase was achieved in the quality factor of the MWCNT-Cu coils (at f =15 MHz). The high aspect ratio and the large surface area of the MWCNT coating was proved to play an important role in the reflection of the external electromagnetic field induced by the current flowing in the adjacent turns, thereby leading to the mitigation of the proximity effect. When MWCNT-Cu coils were used as the transmitter components in the WPT system, efficiencies as high as 95.81% were realized at f = 3.45 MHz. Furthermore, we demonstrated that the proposed method was effective at increasing the available load resistance and transmission range. The improvements achieved in this work were in direct relation with the inductance value of the coils, indicating the potential of MWCNT coatings in improving the performance of the WPT systems.

Acknowledgements

This research activity was financially supported by the National Science Foundation (CMMI 1265122), and by the Nebraska Center for Energy Sciences Research (NCESR). The authors are grateful to Dr. Joe Zhou, Center for Biotechnology, University of Nebraska-Lincoln, for extending the characterization facility and helping with the SEM imaging.

References

[1] T. Chang, Y. Tanabe, B. Tan, A. Poon, Inductive power transfer and farfield radiation with small dual-band antennas, Microwave and Optical Technology Letters 57(5) (2015) 1053-1056.

[2] S. Li, C.C. Mi, Wireless power transfer for electric vehicle applications, IEEE journal of emerging and selected topics in power electronics 3(1) (2015) 4-17.

[3] M. Maso, C. Zhong, X. Zhou, H.A. Suraweera, Wireless-Powered Cooperative Relay Networks, Wiley Encyclopedia of Electrical and Electronics Engineering.

[4] L. Xie, Y. Shi, Y.T. Hou, A. Lou, Wireless power transfer and applications to sensor networks, IEEE Wireless Communications 20(4) (2013) 140-145.

[5] Z. Jia, G. Yan, B. Zhu, Design of a telemetry system based on wireless power transmission for physiological parameter monitoring, AIP Advances 5(4) (2015) 041320.

[6] E.G. Kilinc, C. Baj-Rossi, S. Ghoreishizadeh, S. Riario, F. Stradolini, C. Boero, G. De Micheli, F. Maloberti, S. Carrara, C. Dehollain, A system for wireless power transfer and data communication of long-term bio-monitoring, IEEE Sensors Journal 15(11) (2015) 6559-6569.

[7] A. Trigui, S. Mehri, A. Ammari, J.B.H. Slama, M. Sawan, Prosthetic power supplies, Wiley Encyclopedia of Electrical and Electronics Engineering (2015).

[8] J.C. Lin, A new IEEE standard for safety levels with respect to human exposure to radio-frequency radiation, IEEE Antennas and Propagation Magazine 48(1) (2006) 157-159.

[9] C. Deqing, W. Lifang, L. Chenling, G. Yanjie, The power loss analysis for resonant wireless power transfer, Transportation Electrification Asia-Pacific (ITEC Asia-Pacific), 2014 IEEE Conference and Expo, IEEE, 2014, pp. 1-4.

[10] G.K. Felic, D. Ng, E. Skafidas, Investigation of frequency-dependent effects in inductive coils for implantable electronics, IEEE Transactions on Magnetics 49(4) (2013) 1353-1360.

[11] W.B. Kuhn, N.M. Ibrahim, Analysis of current crowding effects in multiturn spiral inductors, IEEE Transactions on Microwave Theory and Techniques 49(1) (2001) 31-38.

[12] S.-H. Lee, R.D. Lorenz, Surface spiral coil design methodologies for high efficiency, high power, low flux density, large air-gap wireless power transfer systems, Applied Power Electronics Conference and Exposition (APEC), 2013 Twenty-Eighth Annual IEEE, IEEE,

2013, pp. 1783-1790.

[13] I.A. Williamson, T.-A.N. Nguyen, Z. Wang, Suppression of the skin effect in radio frequency transmission lines via gridded conductor fibers, Applied Physics Letters 108(8) (2016) 083502.

[14] M.F. Carias, W. Dominguez-Viqueira, G.E. Santyr, Improving signal-to-noise ratio of hyperpolarized noble gas MR imaging at 73.5 mT using multiturn Litz wire radiofrequency receive coils, Concepts in Magnetic Resonance Part B: Magnetic Resonance Engineering 39(1) (2011) 37-42.

[15] L. Ke, G. Yan, S. Yan, Z. Wang, X. Li, Optimal design of litz wire coils with sandwich structure wirelessly powering an artificial anal sphincter system, Artificial organs 39(7) (2015) 615-626.

[16] T. Mizuno, S. Yachi, A. Kamiya, D. Yamamoto, Improvement in efficiency of wireless power transfer of magnetic resonant coupling using magnetoplated wire, IEEE Transactions on Magnetics 47(10) (2011) 4445-4448.

[17] T. Mizuno, S. Enoki, T. Asahina, T. Suzuki, M. Noda, H. Shinagawa, Reduction of proximity effect in coil using magnetoplated wire, IEEE transactions on magnetics 43(6) (2007) 2654-2656.

[18] Z. Pantic, B. Heacock, S. Lukic, Magnetic link optimization for wireless power transfer applications: modeling and experimental validation for resonant tubular coils, Energy Conversion Congress and Exposition (ECCE), 2012 IEEE, IEEE, 2012, pp. 3825-3832.

[19] M. D'Amore, M. Sarto, A. D'Aloia, Skin-effect modeling of carbon nanotube bundles: The high-frequency effective impedance, Electromagnetic Compatibility (EMC), 2010 IEEE International Symposium on, IEEE, 2010, pp. 847-852.

[20] E.K. Farahani, R. Sarvari, Compact closed form model for skin and proximity effect in multiwall carbon nanotube bundles as GSI interconnects, IEEE Transactions on Electron Devices 61(8) (2014) 2899-2904.

[21] K. Keramatnejad, Y. Gao, Y. Zhou, H. Rabiee Glogir, M. Wang, Y. Lu, Skin Effect Suppression in Infrared-laser Irradiated Planar Multi-walled Carbon Nanotube/Cu Conductors, Proceedings of the 34th International Congress on Applications and Lasers and Electro-Optics (ICALEO), Atlanta, GA, 2015.

[22] K. Keramatnejad, Y.S. Zhou, Y. Gao, H. Rabiee Golgir, M. Wang, L. Jiang, J.-F. Silvain,

Y.F. Lu, Skin effect mitigation in laser processed multi-walled carbon nanotube/copper conductors, Journal of Applied Physics 118(15) (2015) 154311.

[23] O.F. Mousa, Multiscale Multiphysics Modeling, Analysis, and Simulations of Carbon-Nanotube-Based High-Frequency Integrated Power Capacitor, IEEE Trans. Power Electron. 28(9) (2013) 4431-4439.

[24] M. Tahvili, S. Jahanmiri, M. Sheikhi, High-frequency transmission through metallic single-walled carbon nanotube interconnects, International Journal of Numerical Modelling: Electronic Networks, Devices and Fields 22(5) (2009) 369-378.

[25] M. Arjmand, K. Chizari, B. Krause, P. Pötschke, U. Sundararaj, Effect of synthesis catalyst on structure of nitrogen-doped carbon nanotubes and electrical conductivity and electromagnetic interference shielding of their polymeric nanocomposites, Carbon 98 (2016) 358-372.

[26] D. Chung, Carbon materials for structural self-sensing, electromagnetic shielding and thermal interfacing, Carbon 50(9) (2012) 3342-3353.

[27] C. Kostagiannakopoulou, G. Maroutsos, G. Sotiriadis, A. Vavouliotis, V. Kostopoulos, Study on the synergistic effects of graphene/carbon nanotubes polymer nanocomposites, Third International Conference on Smart Materials and Nanotechnology in Engineering, International Society for Optics and Photonics, 2012, p. 840911.

[28] E. Sano, E. Akiba, Electromagnetic absorbing materials using nonwoven fabrics coated with multi-walled carbon nanotubes, Carbon 78 (2014) 463-468.

[29] Z. Zeng, M. Chen, H. Jin, W. Li, X. Xue, L. Zhou, Y. Pei, H. Zhang, Z. Zhang, Thin and flexible multi-walled carbon nanotube/waterborne polyurethane composites with high-performance electromagnetic interference shielding, Carbon 96 (2016) 768-777.

[30] H. Li, K. Banerjee, High-frequency analysis of carbon nanotube interconnects and implications for on-chip inductor design, IEEE Transactions on Electron Devices 56(10) (2009) 2202-2214.

[31] F. Maradei, M. D'Amore, S. Cruciani, M. Feliziani, High quality factor of CNT-based spiral inductors, Electromagnetic Compatibility, Tokyo (EMC'14/Tokyo), 2014 International Symposium on, IEEE, 2014, pp. 469-472.

[32] C. Rutherglen, P. Burke, Nanoelectromagnetics: Circuit and electromagnetic properties of carbon nanotubes, small 5(8) (2009) 884-906.

[33] D.-Y. Kim, Y.S. Yun, H. Bak, S.Y. Cho, H.-J. Jin, Aspect ratio control of acid modified multiwalled carbon nanotubes, Current Applied Physics 10(4) (2010) 1046-1052.

[34] N. Li, Y. Huang, F. Du, X. He, X. Lin, H. Gao, Y. Ma, F. Li, Y. Chen, P.C. Eklund, Electromagnetic interference (EMI) shielding of single-walled carbon nanotube epoxy composites, Nano letters 6(6) (2006) 1141-1145.

[35] C. Deng, G. Zhu, R.D. Lorenz, MHz frequencies, kW, 30 cm gap wireless power transfer with low air gap flux density and high efficiency using surface spiral winding coils, Applied Power Electronics Conference and Exposition (APEC), 2017 IEEE, IEEE, 2017, pp. 1606-1613.

[36] K. Furuta, R. Baba, E. Shun, K. Nunokawa, W. Takahashi, T. Maruyama, Wireless power transmission applied the mutual coupling between coils, AIP Conference Proceedings, AIP Publishing, 2017, p. 070003.

[37] D.H. Tran, W. Choi, Design of a High-Efficiency Wireless Power Transfer System With Intermediate Coils for the On-Board Chargers of Electric Vehicles, IEEE Transactions on Power Electronics 33(1) (2018) 175-187.

[38] M. Lawrence, Y. Jiang, Porosity, pore size distribution, micro-structure, Bio-aggregates Based Building Materials, Springer2017, pp. 39-71.

[39] J.G. Park, J. Louis, Q. Cheng, J. Bao, J. Smithyman, R. Liang, B. Wang, C. Zhang, J.S. Brooks, L. Kramer, Electromagnetic interference shielding properties of carbon nanotube buckypaper composites, Nanotechnology 20(41) (2009) 415702.

[40] B. Singh, V. Choudhary, P. Saini, S. Pande, V. Singh, R. Mathur, Enhanced microwave shielding and mechanical properties of high loading MWCNT–epoxy composites, Journal of nanoparticle research 15(4) (2013) 1554.

[41] N.A. Talwalkar, C.P. Yue, S.S. Wong, Analysis and synthesis of on-chip spiral inductors, IEEE Transactions on electron devices 52(2) (2005) 176-182.

[42] R.J. Calder, S.-H. Lee, R.D. Lorenz, Efficient, MHz frequency, resonant converter for sub-meter (30 cm) distance wireless power transfer, Energy Conversion Congress and Exposition (ECCE), 2013 IEEE, IEEE, 2013, pp. 1917-1924.

[43] Z.N. Low, R.A. Chinga, R. Tseng, J. Lin, Design and test of a high-power high-efficiency loosely coupled planar wireless power transfer system, IEEE transactions on industrial electronics 56(5) (2009) 1801-1812.

[44] F.H. Raab, Effects of circuit variations on the class E tuned power amplifier, IEEE Journal of Solid-State Circuits 13(2) (1978) 239-247.

[45] G.A. Covic, J.T. Boys, Modern trends in inductive power transfer for transportation applications, IEEE Journal of Emerging and Selected topics in power electronics 1(1) (2013) 28-41.

[46] T.P. Duong, J.-W. Lee, Experimental results of high-efficiency resonant coupling wireless power transfer using a variable coupling method, IEEE Microwave and Wireless Components Letters 21(8) (2011) 442-444.

[47] C.J. Stevens, Magnetoinductive waves and wireless power transfer, IEEE Transactions on Power Electronics 30(11) (2015) 6182-6190.

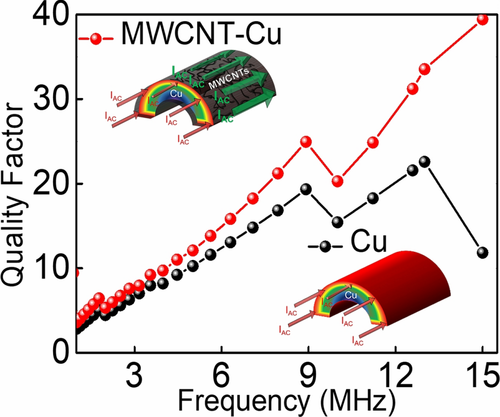

MWCNT-Cu
Cu
MWCNTs
Cu
Cu
Quality Factor
Frequency (MHz)
0
10
20
30
40
3
6
9
12
15